Eur. J. Mineral.
2015, **27**, 123–136
Published online 3 December 2014

# Mayenite supergroup, part III: Fluormayenite, $Ca_{12}Al_{14}O_{32}$ [$\square_4F_2$], and fluorkyuygenite, $Ca_{12}Al_{14}O_{32}[(H_2O)_4F_2]$, two new minerals from pyrometamorphic rocks of the Hatrurim Complex, South Levant

EVGENY V. GALUSKIN[1,*], FRANK GFELLER[2], THOMAS ARMBRUSTER[2], IRINA O. GALUSKINA[1], YEVGENY VAPNIK[3], MATEUSZ DULSKI[4,5], MIKHAIL MURASHKO[6], PIOTR DZIERŻANOWSKI[7], VIKTOR V. SHARYGIN[8,9], SERGEY V. KRIVOVICHEV[10] and RICHARD WIRTH[11]

[1] Department of Geochemistry, Mineralogy and Petrography, Faculty of Earth Sciences, University of Silesia, Będzińska 60, 41–200 Sosnowiec, Poland
*Corresponding author, e-mail: evgeny.galuskin@us.edu.pl
[2] Mineralogical Crystallography, Institute of Geological Sciences, University of Bern, Freiestrasse 3, 3012 Bern, Switzerland
[3] Department of Geological and Environmental Sciences, Ben-Gurion University of the Negev, POB 653, Beer-Sheva 84105, Israel
[4] Institute of Physics, University of Silesia, Uniwersytecka 4, 40–007 Katowice, Poland
[5] Poland and Silesian Center for Education and Interdisciplinary Research, 75 Pułku Piechoty 1a, 41–500 Chorzow, Poland
[6] Systematic Mineralogy, 44, 11th line V.O, apt. 76, Saint Petersburg 199178, Russia
[7] Institute of Geochemistry, Mineralogy and Petrology, Warsaw University, al. Żwirki i Wigury 93, 02–089 Warszawa, Poland
[8] V.S. Sobolev Institute of Geology and Mineralogy, Siberian Branch of the RAS, prosp. Akademika Koptyuga 3, Novosibirsk 630090, Russia
[9] Russia and Department of Geology and Geophysics, Novosibirsk State University, Pirogova Street 2, Novosibirsk 630090, Russia
[10] Department of Crystallography, Geological Faculty, Saint Petersburg State University, University Embankment 7/9, St Petersburg 199034, Russia
[11] Helmholtz Centre Potsdam, GFZ German Research Centre for Geosciences, Section 3.3, Telegrafenberg, 14473 Potsdam, Germany

**Abstract:** Two new mineral species of the mayenite group, fluormayenite $Ca_{12}Al_{14}O_{32}[\square_4F_2]$ ($I\bar{4}3d$, $a = 11.9894(2)$ Å, $V = 1723.42(5)$ Å$^3$, $Z = 2$) and fluorkyuygenite $Ca_{12}Al_{14}O_{32}[(H_2O)_4F_2]$ ($I\bar{4}3d$, $a = 11.966(2)$ Å, $V = 1713.4(1)$ Å$^3$, $Z = 2$), are major constituents of larnite pyrometamorphic rocks of the Hatrurim Complex (Mottled Zone) distributed along the Dead Sea rift on the territory of Israel, Palestinian Autonomy and Jordan. Holotype specimens of fluormayenite and fluorkyuygenite were collected at the Jabel Harmun, Judean Mts., Palestinian Autonomy and in the Hatrurim Basin, Negev Desert, Israel, respectively. Mineral associations of holotype fluormayenite and fluorkyuygenite are similar and include larnite, shulamitite, Cr-containing spinel–magnesioferrite series, ye'elimite, fluorapatite–fluorellestadite, periclase, brownmillerite, oldhamite as well as the retrograde phases portlandite, hematite, hillebrandite, afwillite, foshagite, ettringite, katoite and hydrocalumite. Fluormayenite and fluorkyuygenite crystals, usually $< 20$ μm in size, are colourless, in places with greenish or yellowish tint, the streak is white. Both minerals are transparent with a vitreous lustre; they do not show fluorescence. Fluormayenite and fluorkyuygenite are isotropic and have similar refractive indices: $n = 1.612(3)$ and $n = 1.610(3)$ (589 nm), respectively. The hardness of fluormayenite and fluorkyuygenite is H (Mohs) 5½–6; VHN load 50 g, 771(38) kg mm$^{-2}$; and 5-5½; VHN load 50 g, 712(83) kg m$^{-2}$, respectively. Both minerals have the microporous tetrahedral framework structure characteristic of the mayenite supergroup. In fluormayenite 1/3 of the structural cages are occupied by fluorine. In fluorkyuygenite, in addition to fluorine and negligible amounts of OH, $H_2O$ molecules occupy about 2/3 of the cages. The holotype fluormayenite from Jabel Harmun has the crystal chemical formula $(Ca_{11.951}Na_{0.037})_{\Sigma 11.987}(Al_{13.675}Fe^{3+}_{0.270}Mg_{0.040}Si_{0.009}P_{0.005}S^{6+}_{0.013})_{\Sigma 14.013}O_{31.503}(OH)_{1.492}[\square_{4.581}F_{1.375}Cl_{0.044}]_{\Sigma 6}$, fluorkyuygenite from the Hatrurim Basin has the composition $Ca_{12.034}(Al_{13.344}Fe^{3+}_{0.398}Si_{0.224})_{\Sigma 13.966}O_{32}[(H_2O)_{3.810}F_{1.894}(OH)_{0.296}]_{\Sigma 6}$. Raman spectra of fluormayenite and fluorkyuygenite in the spectral region 200–1000 cm$^{-1}$ are similar and are characterized by the four strong main bands at about 320 ($\nu_2$ $AlO_4$), 520 ($\nu_4$ $AlO_4$), 700, 770 ($\nu_1$ $AlO_4$) cm$^{-1}$. In the O-H vibration region fluorkyuygenite shows a

0935-1221/15/0027-2420 $ 6.30
DOI: 10.1127/ejm/2015/0027-2420

broad band between 2600–3500 $cm^{-1}$ ($\nu H_2O$). The molecular water is completely released from the fluorkyuygenite structure at about 400°C. Fluorkyuygenite crystallized initially as fluormayenite, which later was altered under influence of water vapour-enriched gases during a combustion process. Fluormayenite has been synthesized and fluorkyuygenite is an analogue of the recently discovered chlorkyuygenite, $Ca_{12}Al_{14}O_{32}[(H_2O)_4Cl_2]$, from the Northern Caucasus, Russia.

**Key-words:** fluorkyuygenite; fluormayenite; new mineral; mayenite supergroup; crystal structure; Raman; pyrometamorphic rocks; Hatrurim Complex; Israel.

## Introduction

Mayenite in the pyrometamorphic rocks of the Hatrurim Complex was identified in 1963 in spurrite rocks of the Nahal Ayalon locality (Central Israel). Later it was recognized as a common mineral of spurrite and larnite pyrometamorphic rocks of this Complex (Gross, 1977). It was assumed that mayenite from Israel had the same crystal chemical formula, $Ca_{12}Al_{14}O_{33}$, as the holotype mayenite from altered carbonate xenoliths in volcanic rocks of the Bellerberg, Eifel near Mayen, Germany (Hentschel, 1964). However, a recent re-investigation of mayenite from Eifel showed an end-member composition close to the $Ca_{12}Al_{14}O_{32}Cl_2$ (Galuskin *et al.*, 2012). Investigation of mayenite from different localities of the Hatrurim Complex in Israel revealed that two fluorine-bearing phases, isostructural with mayenite, are widespread in larnite rocks. These phases were studied by our group and were approved by CNMNC IMA in 2013 as new mineral species: fluormayenite $Ca_{12}Al_{14}O_{32}[\square_4F_2]$ (IMA2013-019) and its hydrated analogue fluorkyuygenite $Ca_{12}Al_{14}O_{32}[(H_2O)_4F_2]$ (IMA2013-043) (Galuskin *et al.*, 2013a and b). These names reflect their chemical composition corresponding to chlormayenite $Ca_{12}Al_{14}O_{32}[\square_4Cl_2]$ and chlorkyuygenite $Ca_{12}Al_{14}O_{32}[(H_2O)_4Cl_2]$, which were also found in pyrometamorphic rocks of the Hatrurim Complex (Galuskin *et al*., 2015a, b).

In the present paper, which is the third of a series of four (parts I-IV) on mayenite supergroup minerals published in this issue, the description of two new mineral species is presented: fluormayenite and fluorkyuygenite from holotype specimens collected at the Jabel Harmun, Judean Mountains, Palestinian Autonomy and from the Hatrurim Basin, Negev Desert, Israel, respectively. In the first paper of this series we present a recommended nomenclature for the mayenite supergroup, and also re-define mayenite and discredit brearleyite (Galuskin *et al.*, 2014a). In the second paper a description of the new mineral chlorkyuygenite is given (Galuskin *et al.*, 2014b), whereas in the fourth paper we present new X-ray single-crystal structure data for eltyubyuite (Gfeller *et al.*, 2014).

Type material of fluormayenite is deposited in the collections of the Museum of Natural History in Bern, Bernastrasse 5, 3005 Bern, Switzerland, catalogue number NMBE-42094. Type specimens of the larnite rock containing abundant fluorkyuygenite and shulamitite (portions of the sample no. M4-218; Sharygin *et al.*, 2013) are deposited in the collections of the Mineralogical Museum of St. Petersburg State University, St. Petersburg, Russia, catalogue number 1/19465), and the Central Siberian Geological Museum of the V.S. Sobolev Institute of Geology and Mineralogy, Novosibirsk, Russia, catalogue number VII-87/1.

## Methods of investigation

Crystal morphology and chemical composition of mayenite group minerals and associated minerals were examined using optical microscopes, a Philips XL30 ESEM/EDAX analytical scanning electron microscope (Faculty of Earth Sciences, University of Silesia) and a CAMECA SX100 electron microprobe (Institute of Geochemistry, Mineralogy and Petrology, University of Warsaw). Electron microprobe analyses (EMPA) of fluormayenite and fluorkyuygenite were performed at 15 kV and 10 nA using the following lines and standards: wollastonite - Ca$K\alpha$, Si$K\alpha$; periclase - Mg$K\alpha$; orthoclase - Al$K\alpha$; $Fe_2O_3$ - Fe$K\alpha$; albite - Na$K\alpha$; baryte - S$K\alpha$; tugtupite - Cl$K\alpha$; fluorphlogopite - F$K\alpha$; fluorapatite - P$K\alpha$.

Single-crystal X-ray diffraction studies of fluormayenite and fluorkyuygenite were carried out using Bruker APEX II SMART diffractometers (Mo$K\alpha$, $\lambda = 0.71073$ Å) (Saint-Petersburg University, Russia, and Bern University, Switzerland). The structure was solved by direct methods, with subsequent analyses of difference-Fourier maps, and refined with neutral atom scattering factors using SHELX97 (Sheldrick, 2008). Split positions were refined with common anisotropic atomic displacement parameters.

The Raman investigations were performed using a WITec confocal CRM alpha 300 Raman microscope (Institute of Physics, University of Silesia, Poland). The spectrometer was equipped with an air cooled solid-state laser operating at 532 nm and a CCD detector, which was cooled to 215 K. The laser was coupled to the microscope via a single-mode optical fibre with a diameter of 50 μm. The scattered radiation was focused onto a multi-mode fibre (50 μm diameter) and a monochromator. A dry Olympus MPLAN (50x/0.76NA or 100x/0.5NA) objective was used. Some 15–20 scans with integration times of 10–15 s and a resolution of 3 $cm^{-1}$ were collected and averaged. The monochromator of the spectrometer was calibrated using the Raman scattering line produced by a silicon plate (520.7 $cm^{-1}$). Temperature-dependent Raman spectra were collected in the range of 298–873 K (in steps of 50 K) using a THMS600 heating stage (Linkam Scientific Instruments) with a precision of ± 10 K/min.

## Occurrence and description of fluormayenite and fluorkyuygenite

A weakly hydrated mayenite-group mineral with a composition close to end-member $Ca_{12}Al_{14}O_{32}[\square_4\ F_2]$, fluormayenite, has been discovered at Jabel Harmun in larnite pyrometamorphic rocks belonging to the Hatrurim Complex. The type locality is near the Palestinian village of Nabi Musa situated in the Judean Desert, West Bank, Palestinian Autonomy, Israel (31°46′N 35°26′E). Jabel Harmun is one of several outcrops of the Hatrurim Complex located in the Judean Desert in the vicinity of the Jerusalem–Jericho highway. A description of the geological setting of the Jabel Harmun and also hypotheses on the formation of Hatrurim Complex pyrometamorphic rocks are summarized by Sokol *et al.* (2007, 2008), Geller *et al.* (2012), Novikov *et al.* (2013) and Galuskina *et al.* (2014). Outcrops of the high-temperature rocks are represented by spurrite-, larnite- and gehlenite-bearing rocks. High-temperature rocks are commonly hydrothermally altered at low temperature to ''pseudo-conglomerates'' (the local term; Gross, 1977), which consist of larnite nodules in a matrix of low-temperature hydrous calcium silicates commonly enriched in secondary carbonate. Such nodules are either enclosed in a matrix formed by low-temperature hydrothermal activity or form loose deposits. The new minerals harmunite $CaFe_2O_4$ (IMA2012-045, Galuskina *et al.*, 2014), nabimusaite $KCa_{12}(SiO_4)_4(SO_4)_2O_2F$ (IMA2012-057, Galuskin *et al.*, 2013c) and vapnikite $Ca_3UO_6$ (IMA2013-082; Galuskin *et al.*, 2014c) were recently discovered at this locality.

The F- and Cl-bearing minerals of the mayenite group are widely distributed in larnite rocks of the Jabel Harmun; however, the description in this study is restricted to two typical specimens containing fluormayenite (M. Murashko's and Ye. Vapnik's collections): 12-6-8 (holotype) and 12-6-9 (co-type) (Fig. 1). Minerals associated with fluormayenite are larnite, fluorellestadite–fluorapatite, brownmillerite–srebrodolskite, shulamitite, harmunite, spinel, magnesioferrite, ye'elimite, gehlenite, periclase, ternesite, nabimusaite, oldhamite, barite, vorlanite, vapnikite, chalcocite, covellite and a potentially new mineral, the Ba-analogue of nabimusaite $(Ba,K)Ca_{12}(SiO_4)_4(SO_4)_2O_2(O,F)$.

Fluormayenite forms rounded grains up to 100 μm and a few tetrahedral crystals up to 20 μm in size. Xenomorphic fluormayenite fills interstices between larnite, brownmillerite and fluorellestadite crystals (Fig. 1A). Commonly fluormayenite occurs as inclusions in ye'elimite (Fig. 1B). Fluormayenite easily hydrates to partially or fully transform into fluorkyuygenite and minerals of the grossular–katoite series. Thus fluormayenite occurs as high-temperature relics hosted by other minerals. Our investigations indicate ye'elmite as the most appropriate host mineral for the preservation of fluormayenite.

Fluorkyuygenite was discovered in the Negev Desert (approximately 5 km southeast of the town of Arad, Israel), in the central part of the Hatrurim Basin (31°12′N 35°14′E), one of the most important localities of the Hatrurim Complex (Bentor, 1960; Gross, 1977). The Hatrurim Basin is the type locality of bayerite, bentorite, ye'elimite, grossite, hatrurite and nagelschmidtite (Gross, 1977; Vapnik *et al.*, 2007) and, more recently, for barioferrite $BaFe^{3+}{}_{12}O_{19}$ (Murashko *et al.*, 2011), murashkoite FeP, halamishite $Ni_5P_4$ (*H*), zuktamrurite $Ni_5P_4$ (*O*), negevite $NiP_2$, transjordanite $Ni_2P$ (Britvin *et al.*, 2013a, b), gurimite $Ba_3(VO_4)_2$ (Galuskina *et al.*, 2013); zadovite $BaCa_6[(SiO_4)(PO_4)](PO_4)_2F$ (Galuskin *et al.*, 2013d), aradite $BaCa_6[(SiO_4)(PO_4)](VO_4)_2F$ (Galuskin *et al.*, 2013e) and shulamitite $Ca_3TiFe^{3+}AlO_8$ (Sharygin *et al.*, 2013). Fluorkyuygenite was found as major constituent, possibly primary, in larnite pseudo-conglomerate pyrometamorphic rocks (Sharygin *et al.*, 2013). It forms isometric tris-tetrahedral crystals up to 20–30 μm in size (Fig. 2A, B) showing {211} faces (Fig. 2C). Fluorkyuygenite occurs with larnite, shulamitite, Cr-containing spinel, ye'elimite, fluorapatite, magnesioferrite, periclase, brownmillerite, oldhamite and retrograde phases (portlandite, hematite, hillebrandite, afwillite, foshagite, katoite and hydrocalumite). The mineral associations of holotype fluormayenite and fluorkyuygenite are similar.

Fluormayenite and fluorkyuygenite crystals are usually colourless, sometimes with greenish or yellowish tint, the streak is white. Both minerals are transparent with a vitreous lustre and show no fluorescence. Fluormayenite and fluorkyuygenite are isotropic and have very similar refractive indices: $n = 1.612(3)$ and $n = 1.610(3)$ (589 nm), respectively. They have no cleavage and show irregular fracture. Due to the small grain size the density could not be measured. Instead, densities for fluormayenite and fluorkyuygenite were calculated from composition and unit-cell volume (Table 1, analyses 1 and 3) yielding 2.745 g $cm^{-3}$ and 2.873 g $cm^{-3}$, respectively. The hardness of fluormayenite and fluorkyuygenite is H (Mohs) 5½–6; VHN load 50 g, 771(38) kg $mm^{-2}$ (mean of 11), and 5–5½; VHN load 50 g, 712(83) kg $m^{-2}$(mean of 9), respectively. Compatibility indices (Mandarino, 1979) calculated on the basis of measured refractive indices and calculated densities for fluorkyuygenite $(1 - (Kp/Kc) = 0.011$, and fluormayenite: $1–(Kp/Kc) = –0.068)$ are superior and fair, respectively. The poorer result for fluormayenite may be explained by the observation that the crystal rims are commonly hydrated.

The chemical compositions of fluormayenite and fluorkyuygenite are similar and, without considering the $H_2O$ molecule, these analyses yield the stoichiometry of $Ca_{12}Al_{14}O_{32}(F,Cl,OH)_2$. However, the totals of microprobe analyses of these minerals measured in the same experimental series are strongly different: for fluormayenite, they usually vary within 98–99 wt.%, for fluorkyuygenite they range from 94 to 96 wt.% (Table 1). The structural study of fluormayenite showed (see below) that atypical OH groups are present as described before for chlormayenite (Galuskin *et al.*, 2012), explaining the deviation of analytical totals from 100 %. These OH

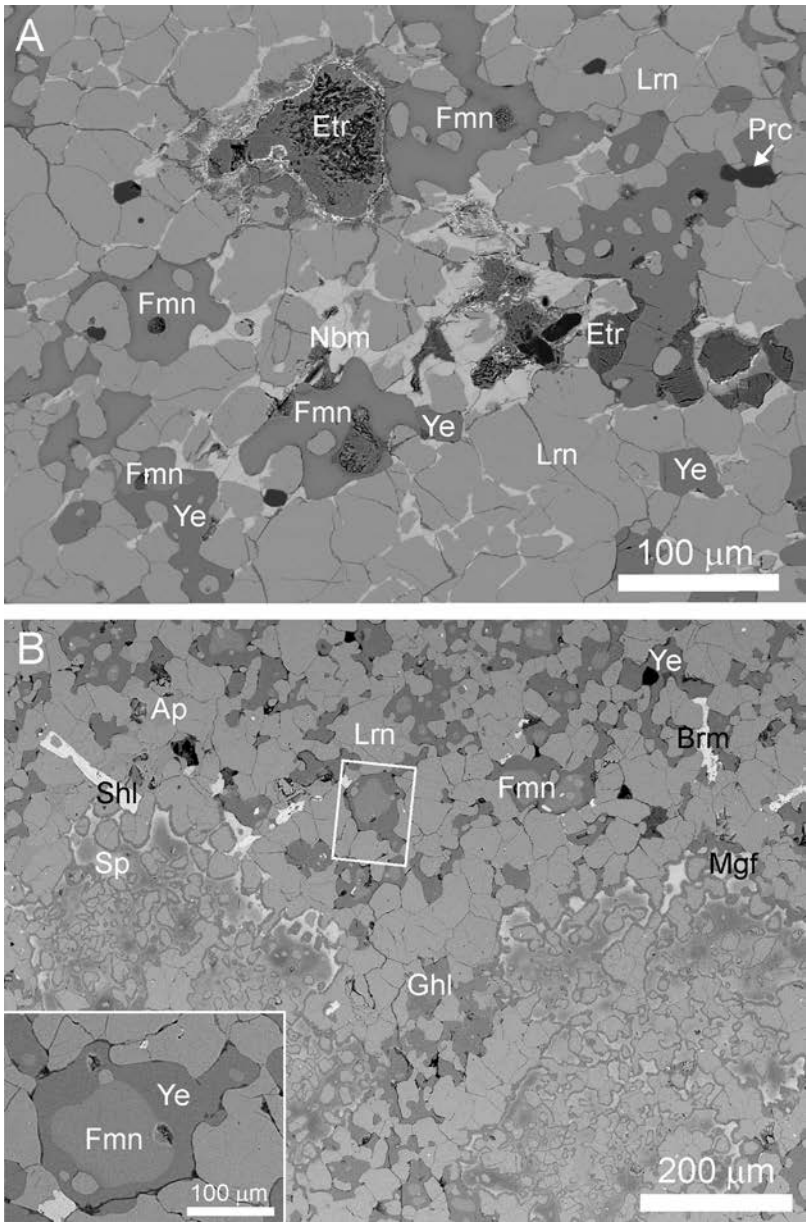


Fig. 1. Backscattered electron images (BSE) of fluormayenite in larnite rocks of the Jabel Harmun. **A**: Fluormayenite from the holotype specimen (no. 12-6-8) represented by xenomorphic grains. **B**: Fluormayenite from the specimen no. 12-6-9 (co-type) represented by rounded grains inside ye'elimite. Area enclosed in the white rectangle is magnified in the inset. Fmn - fluormayenite, Lrn - larnite, Ye - ye'elimite, Nbm - nabimusaite, Prc - periclase, Etr - ettringite, Ap - fluorapatite, Ghl - gehlenite, Brm - brownmillerite, Sp - spinel, Mgf - magnesioferrite, Shl - shulamitite.

groups enter the fluormayenite structure according to the scheme $O^{2-} + {}^{W}F^{-} + {}^{W}2\square = 3(OH)^{-}$ accompanied by a partial change of Al coordination from tetrahedral to octahedral. The theoretical OH end-member of this substitution is $Ca_{12}Al_{14}O_{30}(OH)_6[\square]_6$. It should be emphasized that minor OH groups, substituting for F in the cage at the *W* site, are also present in fluormayenite as shown by the Raman spectrum (Fig. 3). However, this minor substitution was not considered for the crystal chemical formula.

The holotype fluormayenite, $(Ca_{11.951}Na_{0.037})_{\Sigma 11.987}(Al_{13.675}Fe^{3+}_{0.270}Mg_{0.040}Si_{0.009}P_{0.005}S^{6+}_{0.013})_{\Sigma 14.013}O_{31.423}(OH)_{1.731}[\square_{4.581}F_{1.375}Cl_{0.044}]_{\Sigma 6}$, is less ferric and contains more of the $Ca_{12}Al_{14}O_{30}(OH)_6[\square]_6$ hypothetical end-member compared with the co-type fluormayenite $(Ca_{11.969}Na_{0.033})_{\Sigma 12.002}(Al_{13.120}Fe^{3+}_{0.705}Si_{0.162}Mg_{0.011})_{\Sigma 13.998}O_{31.735}(OH)_{0.796}[\square_{4.581}F_{1.814}Cl_{0.037}]_{\Sigma 6}$, which occurs inside ye'elimite grains (Table 1, Fig. 1). The OH content of fluorkyuygenite was calculated based on charge balance. After balancing cation and anion charges the $H_2O$ content was formally calculated using the formula: $H_2O$ pfu $= 6 - (F + Cl + OH)$. In the holotype fluorkyuygenite, $Ca_{12.034}(Al_{13.344}Fe^{3+}_{0.398}Si_{0.224})_{\Sigma 13.966}O_{32}[(H_2O)_{3.810}F_{1.894}(OH)_{0.296}]_{\Sigma 6}$, the hypothetical end-member $Ca_{12}Al_{14}O_{32}[(H_2O)_4(OH)_2]$ contributes to its composition by 14 %

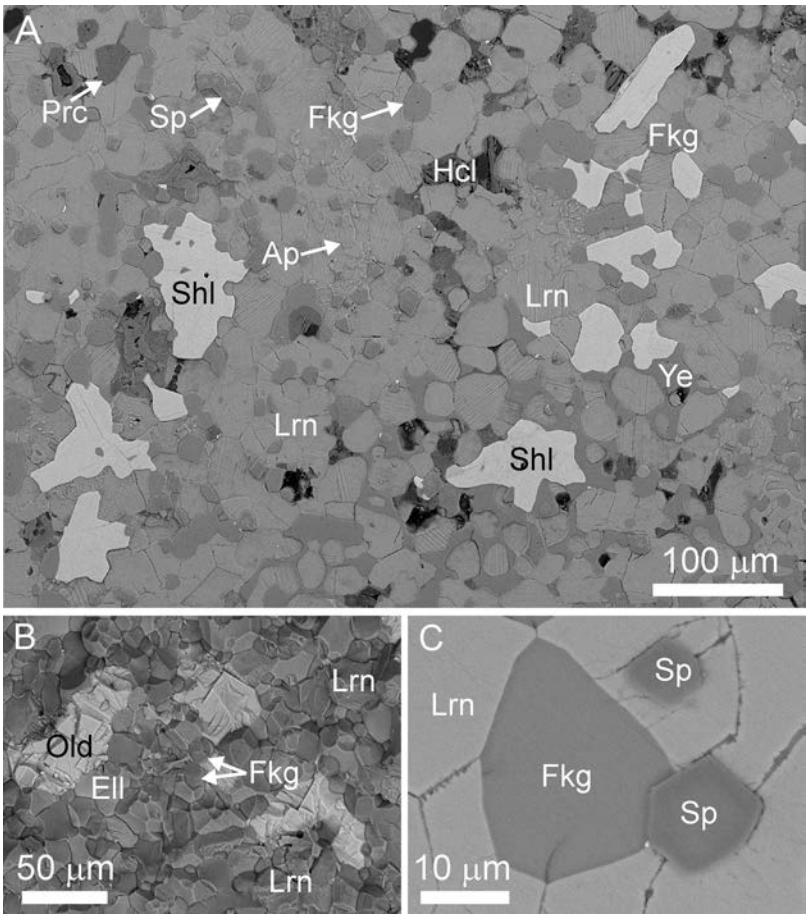


Fig. 2. BSE images of fluorkyuygenite in larnite rocks of the Hatrurim Basin, holotype specimen no. M4-218 of shulamitite and fluorkyuygenite. **A**: Image of the same thin-section after polishing, which was already shown for the description of shulamitite by Sharygin *et al.* (2013); polysynthetic twinning of larnite is well visible. **B**: Fractured sample surface without conductive coating. Rounded grains of fluorkyuygenite in oldhamite-enriched rock, low vacuum, 0.3 Torr. **C**: tris-tetrahedral fluorkyuygenite crystal. Fkg - fluorkyuygenite, Lrn - larnite, Ye - ye'elimite, Prc - periclase, Hcl - hydrocalumite, Ap - fluorapatite, Ell - fluorellestadite, Sp - spinel, Shl - shulamitite, Old - oldhamite.

(Table 1) suggesting the possibility of finding hydrated analogues of fluor- and chlorkyuygenite in nature.

## Raman and structural investigations of fluormayenite and fluorkyuygenite

The main bands on the Raman spectra of the mayenite-group minerals are related to Al–O vibrations at $(AlO_4)^{5-}$ tetrahedra and O–H stretching vibrations of hydroxyl groups $(OH)^-$ and $H_2O$ molecules (Table 2, Fig. 3). Chlor- and fluorkyuygenite differ from chlor- and fluormayenite by the presence of a broad band in the range of O–H stretching vibrations, which are interpreted as being caused by $H_2O$ molecules (Fig. 3, Galuskin *et al.*, 2014b). The broad band 2600–3500 $cm^{-1}$ with two weakly expressed maxima at about 3020 and 3200 $cm^{-1}$ in the fluorkyuygenite spectrum is shifted towards lower frequencies compared with chlorkyuygenite (Galuskin *et al.*, 2014b). Bands at 3560–3580 $cm^{-1}$, which are related to OH groups substituting for F (Cl) at the central *W* site (Galuskin *et al.*, 2012; Dulski *et al.*, 2014), also appear on the spectra of fluor- and chlormayenite (Fig. 3). Bands at 3670–3680 $cm^{-1}$ are related to OH groups, in chlor- and fluormayenite according to the scheme: $O^{2-} + {}^{W}F/Cl^- \rightarrow 3(OH)^-$ defining a partial coordination change of Al from tetrahedral to octahedral (Galuskin *et al.*, 2012; Dulski *et al.*, 2014; Fig. 3).

Temperature-dependent Raman experiments showed that ''zeolitic'' water in the structural cages of fluorkyuygenite remained up to about 400°C (Fig. 4). In chlorkyuygenite the ''zeolite'' water is released at 550°C (Galuskin *et al.*, 2014b). In the spectrum of fluorkyuygenite heated up to 400°C, a new band at about 3560 $cm^{-1}$ occurred, which was assigned to OH at the *W* site. This band was not observed in the spectra of unheated fluorkyuygenite (Fig. 4). Calculated on the basis of charge balance OH groups occupy about 10 % of the *W* site in the holotype fluorkyuygenite (Table 1).

At temperatures lower than −100°C two expressed maxima at about 3100 and 3220 $cm^{-1}$ are observed in the fluorkyuygenite spectrum. These bands are analogous to

Table 1. Chemical composition (in wt.%) of fluormayenite and fluorkyuygenite from pyrometamorphic rocks of the Hatrurim Complex.

| Specimen | 12-6-8 | s.d. | range | 12-6-9 | M4-218 | s.d. | range |
|---|---|---|---|---|---|---|---|
| $SiO_2$ | 0.04 | 0.02 | 0.02–0.08 | 0.67 | 0.89 | 0.3 | 0.44–1.41 |
| $Al_2O_3$ | 48.85 | 0.2 | 48.2–49.1 | 46.0 | 45.00 | 0.3 | 44.4–45.4 |
| $Fe_2O_3$ | 1.51 | 0.11 | 1.32–1.75 | 3.87 | 2.10 | 0.4 | 1.59–2.68 |
| MgO | 0.11 | 0.02 | 0.08–0.15 | 0.03 | <0.02 | | |
| CaO | 46.96 | 0.1 | 47.4–47.8 | 46.2 | 44.64 | 0.3 | 44.0–45.2 |
| $Na_2O$ | 0.08 | 0.01 | 0.06–0.10 | 0.07 | <0.02 | | |
| $SO_3$ | 0.08 | 0.03 | 0.04–0.12 | <0.03. | <0.03 | | |
| $P_2O_5$ | 0.03 | 0.03 | <0.03–0.06 | <0.03 | <0.03 | | |
| Cl | 0.11 | 0.01 | 0.09–0.12 | 0.09 | <0.02 | | |
| F | 1.83 | 0.2 | 1.58–2.11 | 2.37 | 2.38 | 0.3 | 1.84–2.84 |
| $H_2O$ | 1.09 | | | 0.49 | 4.72 | | |
| $-O = F + Cl$ | 0.80 | | | 1.02 | 1.00 | | |
| Total | 99.88 | | | 98.7 | 98.72 | | |
| calculated on 26 cations | | | | | | | |
| Ca | 11.951 | | | 11.969 | 12.034 | | |
| Na | 0.037 | | | 0.033 | | | |
| X | **11.987** | | | **12.002** | **12.034** | | |
| Al | 13.675 | | | 13.120 | 13.344 | | |
| $Fe^{3+}$ | 0.270 | | | 0.705 | 0.398 | | |
| Si | 0.009 | | | 0.162 | 0.224 | | |
| Mg | 0.040 | | | 0.011 | | | |
| $S^{6+}$ | 0.013 | | | | | | |
| P | 0.005 | | | | | | |
| Z | **14.013** | | | **13.998** | **13.966** | | |
| F | 1.375 | | | 1.814 | 1.894 | | |
| Cl | 0.044 | | | 0.037 | | | |
| OH* | | | | | 0.296 | | |
| $H_2O$** | | | | | 3.810 | | |
| W | **1.419** | | | **1.851** | **6.000** | | |
| OH*** | 1.731 | | | 0.796 | | | |
| $Ca_{12}Al_{14}O_{32}[\square_4F_2]$ | 69 % | | | 82 % | | | |
| $Ca_{12}Al_{14}O_{32}[(H_2O)_4F_2]$ | | | | | 81 % | | |
| $Ca_{12}Al_{14}O_{30}(OH)_6$ theor. | 29 % | | | 13 % | | | |
| $Ca_{12}Al_{10}Si_4O_{32}F_6$ theor. | | | | 4 % | 5 % | | |
| $Ca_{12}Al_{14}O_{32}[(H_2O)_4(OH)_2]$ theor | | | | | 14 % | | |
| others | 2 % | | | 1 % | | | |
| $Al = Al + Fe^{3+}$ (Al>> Fe), $F = F + Cl$ ($F$ >> Cl) | | | | | | | |

*Footnote: n.d. – not detected.*

the zero-dimension ice bands (Garcia *et al.*, 2006; Kolesov, 2006).

The crystal structures of fluormayenite and fluorkyuygenite were refined in space group $I\bar{4}3d$, and corresponding structural data are presented in Tables 3–8. Minerals of the mayenite group have a zeolite-like structure with a $\{Al_{14}O_{32}\}^{22-}$ tetrahedral framework enclosing six big cages (~5 Å) each occupied by two $Ca^{2+}$, which leads to an excess of two positive charges. At the centre of the cage (*W* site) anions balance the charge of the framework and Ca (Fig. 5).

The structure refinement of a fluormayenite (a single crystal of specimen 12-6-8) resulted in the formula $Ca1_{9.108}Ca1a_{2.892}Al1_8Al2_6O1_{24}O2_{7.08}(O2aH)_{2.76}$ $[\square_{4.554}F_{1.446}]$ or simply $Ca_{12}Al_{14}O_{31.08}(OH)_{2.76}[\square_{4.554}F_{1.446}]$ with cation and anion charge sums of: (+66) and (–66.37) (Table 4), respectively. The following occupancy constraints were applied in the refinement: occ. Ca*1a* = occ. OH/F at *W*; occ. Ca*1* = 1 − occ. Ca*1a*; occ. O*2* = 1 − occ. O*2a*. The small excess of negative charge can be explained by negligible impurities of highly charged elements at the Al sites, such as Si, $S^{6+}$, P. Moreover, minor Cl may contribute to the electron density at the *W* site, which has been refined as F. The simplified crystal chemical formula of the holotype fluormayenite, $Ca_{12}Al_{14}O_{31.42}(OH)_{1.73}[\square_{4.57}F_{1.43}]$, calculated on the basis of electron microprobe data (Table 1), differs from the formula derived from the structure refinement by the amount of OH groups substituting according to the scheme $^{O2}O^{2-} + {}^{W}F/Cl^{-} + {}^{W}2\square \rightarrow {}^{O2a}3(OH)^{-} + {}^{W}3\square$. Electron microprobe analyses were generally performed at the central, less hydrated part of the grains. The small size of fluormayenite grains did not allow performing single-crystal X-ray experiments of a completely unaltered sample.

Structural data on fluorkyuygenite were obtained from a very small crystal about 20 μm in size (Table 3). The crystal chemical formula obtained by site population refinements, considering the cavity O as $H_2O$ was $Ca1_{7.92}Ca1a_{4.08}Al1_{7.552}Fe1_{0.448}Al2_6O1_{24}O2_8[F_{2.03}(H_2O)_{3.79}]$ yielding cation and anion charge sums of (+66) and (–66.03) (Table 5),

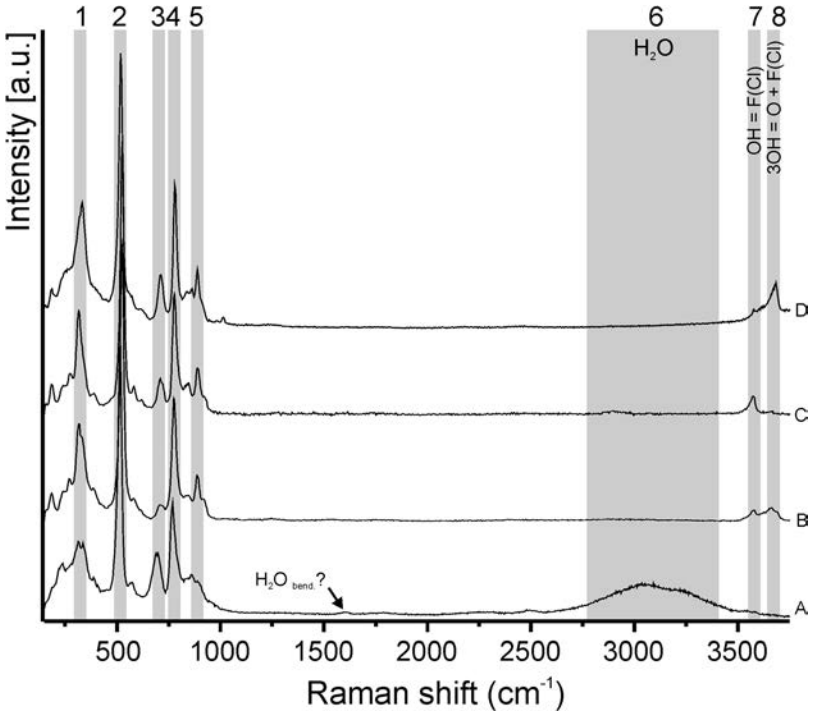


Fig. 3. Raman spectra of mayenite-group minerals. A: fluorkyuygenite, crystal in Fig. 2C. B, C: fluormayenite, crystal in Fig.1B (inset): B – rim, C – core. D: chlormayenite, grain from holotype specimen no. M5026/86, Mineral Museum, University of Cologne, Cologne. Grey lines show positions of the main bands.

Table 2. Main Raman bands of mayenite group minerals ($cm^{-1}$).

| | | Fluormayenite | Fluorkyuygenite | Chlorkyuygenite | Chlormayenite |
|---|---|---|---|---|---|
| | *a*, Å | 11.989(1) | 11.966(2) | 12.029(1) | 12.032(1) |
| | number on Fig. 3 | | | | |
| $\nu_2$ $(AlO_4)^{5-}$ | 1 | 318 | 344<br>320 | 321 | 331 |
| $\nu_4$ $(AlO_4)^{5-}$ | 2 | 524 | 517 | 511 | 520 |
| $\nu_1$ $(AlO_4)^{5-}$ | 3 | 709 | 695 | 705 | 712 |
| | 4 | 776 | 772 | 779 | 781 |
| $\nu_3$ $(AlO_4)^{5-}$ | 5 | 890 | 898 | 881 | 891 |
| ν (HOH) | 6 | | 2600–3500 | 2750–3600 | |
| ν $(OH)^-$ | 7 | 3572 | | | 3564 |
| | 8 | 3674 | | | 3685 |

respectively. In these refinements the split Ca sites Ca*1* and Ca*1a* were refined with constrained occupancies: occ. Ca*1a* = occ. F at *W*; occ. Ca*1* = 1 – occ. Ca*1a*. The occupancy of additional $H_2O$ at *W* was refined without constraint but displacement parameters of $H_2O$ and F at *W* were set equal. The EMPA data disclosed that small amounts of Si substitute for Al (Table 1). The scattering factors of Al and Si are too similar to be distinguished by Mo *Kα* radiation X-ray structure refinement. The Si-corrected crystal chemical formula becomes charge balanced, $Ca_{12}Al_{13.33}Fe^{3+}_{0.45}Si_{0.22}O_{32}[(H_2O)_{3.60}F_{2.03}(OH)_{0.19}]_{\Sigma 5.82}$, if some $H_2O$ is interpreted as the cavity OH. This revised formula is similar to $Ca_{12.034}(Al_{13.344}Fe^{3+}_{0.398}Si_{0.224})_{\Sigma 13.966}O_{32}[(H_2O)_{3.810}F_{1.894}(OH)_{0.296}]_{\Sigma 6}$ which has been obtained from results of microprobe analyses.

The structural investigation of chlorkyuygenite $Ca_{12}Al_{14}O_{32}[(H_2O)_4Cl_2]_{\Sigma 6}$ from Northern Caucasus indicates that $H_2O$ molecules occupy the same central *W* site as Cl (Galuskin *et al.*, 2014b). While chlorkyuygenite has one well defined Ca site, in fluorkyuygenite Ca is split into two sub-sites, Ca*1*, occupancy 0.661(17), and Ca*1a*, occupancy 0.349(17). Corresponding splitting is evident in fluormayenite: Ca*1* (occupancy 0.76) and Ca*1a* (0.24) (Fig. 5, Tables 4, 5 and 8). Both sites are *ca.* 0.4 Å apart. The origin of the Ca splitting is $F^-$([$OH^-$]) at *W* sites attracting Ca*1a*. Thus the occupancy of F at *W* was constrained to Ca*1a* occupancy. Compared to the empty cages in fluormayenite, fluorkyuygenite shows cages filled with $H_2O$. The Ca*1*–Ca*1* distances of empty cages in fluormayenite (5.64 Å) are significantly longer compared to the Ca*1*–Ca*1* distances in

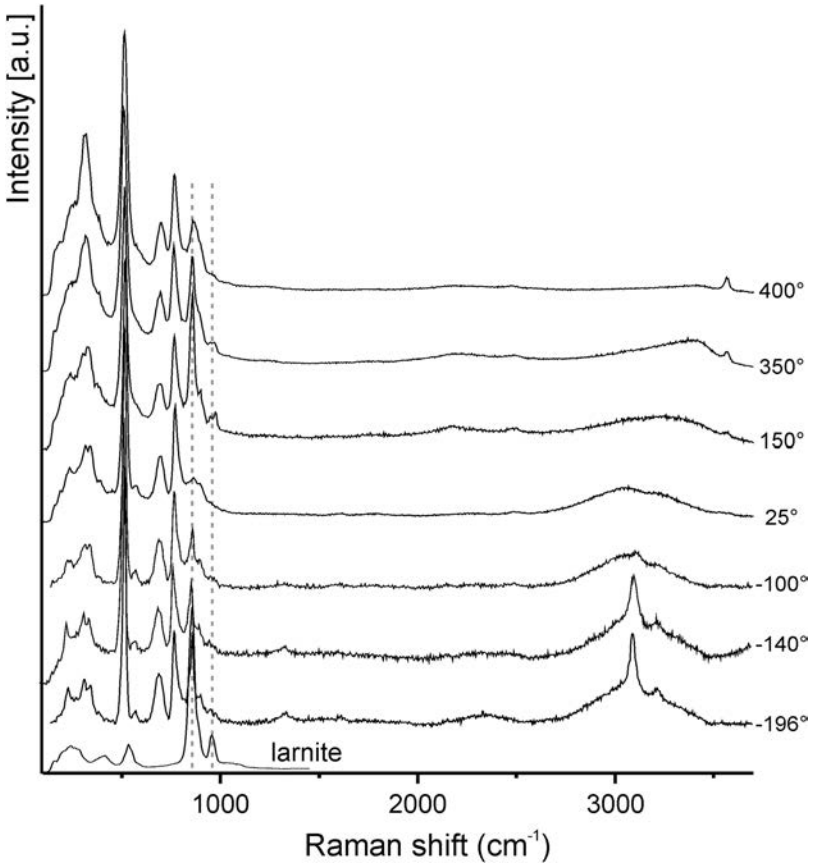


Fig. 4. Raman spectra of fluorkyuygenite at different temperatures. Due to the experimental conditions we could not avoid interference from adjacent larnite in the recorded spectra. For comparison the larnite spectrum is also shown.

fluorkyuygenite (5.28 Å). Thus the cage-filling $H_2O$ molecules also attract the adjacent Ca*1* sites. A corresponding observation has been made for chlormayenite and chlorkyuygenite showing Ca – Ca separations of 5.71 Å and 5.46 Å, respectively (Galuskin *et al.*, 2014b).

The residual density at *W* in the fluorkyuygenite structure due to additional $H_2O$ was also refined ($H_2O$) with oxygen scattering factors and common $U_{ij}$ values for F and $H_2O$ at *W*. The sum of $H_2O$ and F adds up to 0.97(5), which is close to full occupancy: 3.79 O ($H_2O$) + 2.03 F (+OH); these numbers are close to those calculated from EMPA results (3.81 O $(H_2O)_{calc.}$ + 2.19[$(F_{1.89}$ + $(OH_{0.30})_{calc.}$]).

Powder X-ray diffraction data could not be obtained due to the difficulty in separating very small grains of fluorkyuygenite and fluormayenite and because it was not possible to distinguish macroscopically between bulk fluormayenite and fluorkyuygenite. Calculated powder diffraction data for fluormayenite and fluorkyuygenite (Cu$K\alpha$) are given in Table 9.

## Discussion

The synthetic analogue of fluormayenite, $Ca_{12}Al_{14}O_{32}$ [$\square_4F_2$], $a \approx 12$ Å, $I\bar{4}3d$, $Z = 2$, is known (Williams, 1973; Qujiun *et al.*, 1997; Huang *et al.*, 2012). The main structural difference of fluormayenite compared to its artificial analogue are additional OH sites according to the substitution O2 $\rightarrow 3 \times$ O2*a* [$^{O2}O^{2-}$ + $^{W}F/Cl^{-}$ + $^{W}2\square \rightarrow$ $^{O2a}3(OH)^{-}$ + $^{W}3\square$] (Table 4). This substitution changes the coordination of Al*1* from tetrahedral to octahedral (Fig. 6). Analogous phenomena were described in the case of partially hydroxylated chlormayenite from the Eifel district (Germany), with the general crystal chemical formula $Ca_{12}Al_{14}O_{32-x}(OH)_{3x}[Cl_{2-x}]$ (x $\sim$ 0.75) (Galuskin *et al.*, 2012). Structural, Raman spectroscopic and chemical investigations show that the general crystal chemical formula of fluormayenite may be written as being in analogy to chlormayenite: $Ca_{12}Al_{14}O_{32-x}(OH)_{3x}[F_{2-x}]$ with x $\approx$ 0.25–0.5 (Table 1). A negligible part of $(OH)^{-}$ may be substituted by $F^{-}$ groups.

The main difference between fluormayenite, $Ca_{12}Al_{14}O_{32}[\square_4F_2]$, and fluorkyuygenite, $Ca_{12}Al_{14}O_{32}$ $[(H_2O)_4F_2]$, is the presence of four additional neutral $H_2O$ molecules in the cages of the latter. This ''space-filling'' $H_2O$ does not influence the cell parameter of the mayenite-type structure (Table 3). However, it shows a pronounced influence on the position of the Ca*1* site since the cage-filling $H_2O$ molecules attract the adjacent Ca.

There are three main mechanisms of water incorporation into the structure of essentially anhydrous minerals of the mayenite group: (1) $^{W}F^{-}(Cl) \rightarrow {}^{W}OH^{-}$, (2) $^{W}\square \rightarrow H_2O$,

Table 3. Data collection and structure refinement details for Fluormayenite and Fluorkyuygenite.

| Crystal data | fluormayenite | fluorkyuygenite |
|---|---|---|
| Unit-cell dimensions (Å) | $a = 11.9894(2)$ | $a = 11.966(2)$ |
| Space group | $I\bar{4}3d$ (No. 220) | |
| Volume (Å$^3$) | 1723.42(5) | 1713.4(1) |
| $Z$ | 2 | |
| Chemical formula | $Ca_{12}Al_{14}O_{31.08}(OH,F)_{2.76}[OH/F_{1.45}]$ | $Ca_{12}Al_{14}O_{32}[(F,OH)_{2.03}(H_2O)_{3.79}]$ |
| Crystal shape | prism | rounded grain |
| Crystal size (mm) | $0.1 \times 0.08 \times 0.08$ | 0.02 |
| Diffractometer | APEX II BRUKER SMART | |
| X-ray radiation | Mo $K\alpha$ | |
| X-ray power | 50 kV 30 mA | |
| Monochromator | Graphite | |
| Temperature | 293 K | |
| Detector to sample distance | 5.95 cm | |
| Measurement method | Phi and Omega scans | |
| Radiation width | 0.5° | |
| Time per frame | 30 s | |
| Max. θ°-range for Data collection | 32.02 | 26.27 |
| Index ranges | $-19 \leq h \leq 19$<br>$-15 \leq k \leq 19$<br>$-17 \leq l \leq 10$ | $-14 \leq h \leq 14$<br>$-14 \leq k \leq 13$<br>$-14 \leq l \leq 14$ |
| No. of measured reflections | 10826 | 7851 |
| No. of unique reflections | 701 | 297 |
| No. of observed reflections ($I > 2\sigma$ (I)) | 686 | 280 |
| Refinement of the structure | | |
| No. of parameters used in refinement | 32 | 29 |
| *R*int | 0.0389 | 0.122 |
| *R*σ | 0.021 | 0.03 |
| *R*1, $I > 2\sigma$(I) | 0.0302 | 0.0274 |
| *R*1 all Data | 0.0309 | 0.031 |
| w*R*2 on (F2) | 0.0765 | 0.0526 |
| GooF | 1.212 | 1.117 |
| Δρ min (-e.Å$^{-3}$) | −0.39 close to O1 | −0.22 close to Ca1a |
| Δρ max (e.Å$^{-3}$) | 0.48 close to Al1 | 0.21 close to O2 |

Table 4. Atom coordinates, $U_{eq}$ (Å$^2$) values, and occupancies for fluormayenite.

| Site | Atom | *x* | *y* | *z* | *U*eq | Occ. |
|---|---|---|---|---|---|---|
| Ca*1** | Ca | 0.13974(9) | 0.0000 | 0.2500 | 0.01153(17) | 0.759(2) |
| Ca*1a** | Ca | 0.1835(3) | 0.0000 | 0.2500 | 0.01153(17) | 0.241(2) |
| *T1* | Al | 0.26832(5) | 0.26832(5) | 0.26832(5) | 0.00754(17) | 1 |
| *T2* | Al | 0.1250 | 0.5000 | 0.2500 | 0.0079(2) | 1 |
| O*1* | O | 0.30716(13) | 0.21386(13) | 0.40079(14) | 0.0150(3) | 1 |
| O*2*** | O | 0.18567(13) | 0.18567(13) | 0.18567(13) | 0.0114(6) | 0.885(9) |
| O*2a*** | OH/F | 0.121(3) | 0.218(4) | 0.296(4) | 0.102(17) | 0.115(9) |
| *W** | OH/F | 0.3750 | 0.0000 | 0.2500 | 0.020(2) | 0.241(2) |

*Footnotes*: * Occupancies of Ca*1* and Ca*1a* are refined due to site splitting driven by OH/F in the centre of structural cages at the *W* site. **Occupancy of O2 is refined due to substitution O2 → 3 × OH.

(3) $^{O2}O^{2-} + {}^{W}F/Cl^{-} + {}^{W}2\square \rightarrow {}^{O2a}3(OH)^{-} + {}^{W}3\square$. Synthetic mayenite, $Ca_{12}Al_{14}O_{32}[\square_5O]$, reacts with water vapour at high temperature (950–1350°C) forming phases of $Ca_{12}Al_{14}O_{32}[\square_4(OH)_2]$ composition. During heating of $Ca_{12}Al_{14}O_{32}[\square_4(OH)_2]$ in dry atmosphere at temperatures > 1100°C, $OH^-$ ions are substituted by different radicals of O (Hayashi *et al.*, 2005). Above 500°C, the $(OH)^-$ ion in $Ca_{12}Al_{14}O_{32}[\square_4(OH)_2]$ may partially be exchanged by F and Cl with formation of the solid-solution series $Ca_{12}Al_{14}O_{32}[\square_4(F,OH)_2]$ and $Ca_{12}Al_{14}O_{32}[\square_4(Cl,OH)_2]$, respectively (Sango, 2006). Small amounts of OH groups at the *W* site occur in fluorkyuygenite and in fluormaynite, as confirmed by our Raman studies (Fig. 3).

In chlorkyuygenite the $H_2O$ molecule at the *W* site is only connected by very weak hydrogen bonds to

Table 5. Atom coordinates, $U_{eq}$ (Å$^2$) values, and occupancies for fluorkyuygenite.

| Site | Species | *x* | *y* | *z* | $U_{eq}$ | Occ. |
|---|---|---|---|---|---|---|
| Ca*1** | Ca | 0.1546(7) | 0 | 0.25 | 0.0125(10) | 0.661(17) |
| Ca*1a** | Ca | 0.1877(7) | 0 | 0.25 | 0.0125(10) | 0.339(17) |
| *T1* | Al | 0.27006(8) | 0.27006(8) | 0.27006(8) | 0.0087(5) | 0.944(6) |
| | Fe | 0.27006(8) | 0.27006(8) | 0.27006(8) | 0.0087(5) | 0.056(6) |
| *T2* | Al | 0.125 | 0.5 | 0.25 | 0.0093(5) | 1 |
| O*1* | O | 0.3077(2) | 0.2122(3) | 0.3997(2) | 0.0350(9) | 1 |
| O2 | O | 0.1870(2) | 0.1870(2) | 0.1870(2) | 0.0121(9) | 1 |
| *W** | F | 0.375 | 0 | 0.25 | 0.0339(19) | 0.339(17) |
| *W* | $H_2O$ | 0.375 | 0 | 0.25 | 0.0339(19) | 0.63(3) |

*Footnote*: * Occupancies of *Ca1* and *Ca1a* are refined due to site splitting driven by OH/F in the centre of structural cages at the *W* site.

Table 6. Anisotropic displacement parameters (Å$^2$) for fluormayenite.

| Site | $U_{11}$ | $U_{22}$ | $U_{33}$ | $U_{23}$ | $U_{13}$ | $U_{12}$ |
|---|---|---|---|---|---|---|
| Ca*1* | 0.0138(4) | 0.0120(2) | 0.0088(2) | 0.00028(19) | 0.000 | 0.000 |
| Ca*1a* | 0.0138(4) | 0.0120(2) | 0.0088(2) | 0.00028(19) | 0.000 | 0.000 |
| *T1* | 0.00754(17) | 0.00754(17) | 0.00754(17) | 0.00119(17) | 0.00119(17) | 0.00119(17) |
| *T2* | 0.0071(4) | 0.0083(3) | 0.0083(3) | 0.000 | 0.000 | 0.000 |
| O*1* | 0.0115(6) | 0.0173(6) | 0.0163(7) | 0.0082(5) | -0.0034(5) | -0.0044(4) |
| O2 | 0.0114(6) | 0.0114(6) | 0.0114(6) | -0.0020(5) | -0.0020(5) | -0.0020(5) |
| *W* | 0.003(3) | 0.028(3) | 0.028(3) | 0.000 | 0.000 | 0.000 |

Table 7. Anisotropic displacement parameters (Å$^2$) for fluorkyuygenite.

| Site | $U_{11}$ | $U_{22}$ | $U_{33}$ | $U_{23}$ | $U_{13}$ | $U_{12}$ |
|---|---|---|---|---|---|---|
| Ca*1* | 0.015(3) | 0.0106(6) | 0.0118(6) | 0.0008(5) | 0.000 | 0.000 |
| Ca*1a* | 0.015(3) | 0.0106(6) | 0.0118(6) | 0.0008(5) | 0.000 | 0.000 |
| *T1* | 0.0087(5) | 0.0087(5) | 0.0087(5) | 0.0018(4) | 0.0018(4) | 0.0018(4) |
| *T2* | 0.0065(9) | 0.0107(6) | 0.0107(6) | 0.000 | 0.000 | 0.000 |
| O*1* | 0.0288(17) | 0.0454(19) | 0.0310(16) | 0.0311(13) | -0.0198(12) | -0.0246(14) |
| O2 | 0.0121(9) | 0.0121(9) | 0.0121(9) | 0.0015(10) | 0.0015(10) | 0.0015(10) |
| *W* | 0.014(3) | 0.044(3) | 0.044(3) | 0.000 | 0.000 | 0.000 |

Table 8. Selected interatomic distances (Å) for fluormayenite and fluorkyuygenite.

| Fluormayenite | | | Fluorkyuygenite | | |
|---|---|---|---|---|---|
| Ca*1* | -O*1* | 2.356(2) 2× | Ca*1* | -O*1* | 2.345(3) 2 × |
| | -O*1* | 2.511(2) 2× | | -O2 | 2.393(2) 2 × |
| | -O2* | 2.419(1) 2× | | -*W* | 2.638(8) |
| | *mean* | 2.429 | | -O*1* | 2.686(8) 2 × |
| | -O2*a** | 2.40(5) 2× | | *mean* | 2.498 |
| | -O2*a** | 2.68(5) 2× | | | |
| | *mean* | 2.487 | Ca*1a* | -*W* | 2.241(9) |
| Ca*1a* | -*W* | 2.296(4) | | -O2 | 2.361(2) 2 × |
| | -O*1* | 2.385(2) 2× | | -O*1* | 2.388(4) 2 × |
| | -O*1* | 2.969(4) 2× | | -O*1* | 3.033(4) 2 × |
| | -O2 | 2.356(1) 2× | | *mean* | 2.544 |
| | *mean* | 2.531 | | | |
| Al*1* | -O*1* | 1.779(2) 3× | Al*1* | -O*1* | 1.758(3) 3 × |
| | -O2* | 1.716(3) | | -O2 | 1.721(5) |
| | *mean* | 1.763 | | *mean* | 1.749 |
| | -O2*a** | 1.90(4) 3× | | | |
| | *mean* | 1.840 | | | |
| Al2 | -O*1* | 1.738(2) 4× | Al2 | -O*1* | 1.734(3) 4 × |

*Footnote*: * Either O2 or O2a is occupied.

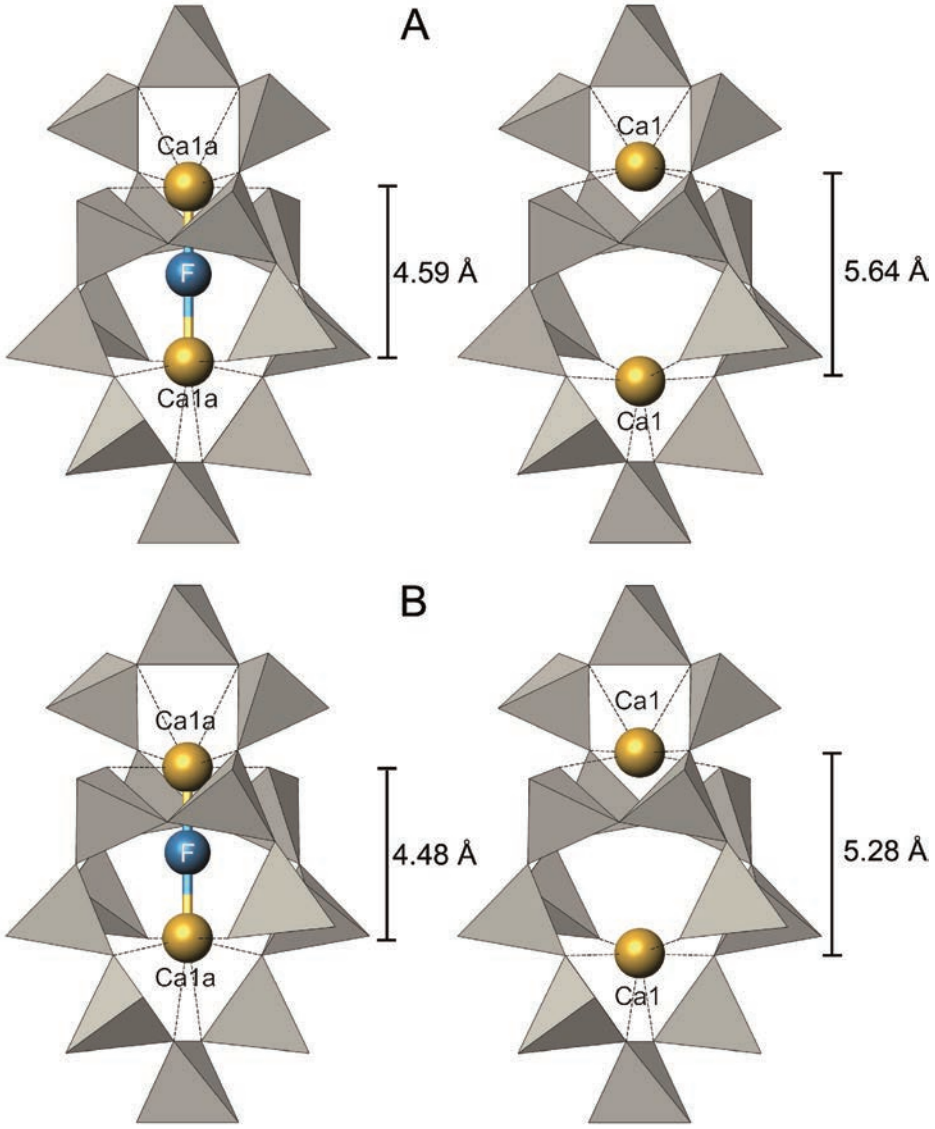


Fig. 5. Comparison of an occupied and an empty cage, built by the grey $AlO_4$-framework tetrahedra in fluormayenite (A) and fluorkyuygenite (B). In both cases the Ca – Ca distances for cages occupied by F are shortened about 0.4–0.5 Å due to the anionic charge. Fluorkyuygenite shows a significantly shorter Ca – Ca distance (5.28 Å) for F-free cages compared to fluormayenite (5.64 Å), indicating that $H_2O$ has a pronounced influence on the actual position of Ca*1*.

framework oxygen sites (O*1* and O2) with $d_{W\text{-}O1,\ O2} > 3.25$ Å (Galuskin *et al.*, 2014b). The corresponding *W* framework oxygen distance $d_{W\text{-}O1,\ O2}$ in fluorkyuygenite is slightly shortened by ~0.03–0.04 Å compared to chlorkyuygenite (Galuskin *et al.*, 2014b). On the other hand, the broad band in Raman spectra of fluorkyuygenite, caused by O–H stretching vibrations in $H_2O$, is shifted *ca.* 150 $cm^{-1}$ towards lower frequencies compared with the corresponding band in the chlorkyuygenite spectrum (Fig. 3, Galuskin *et al.*, 2014b). It is not trivial to predict the real configuration of the hydrogen bond system O···H-O*3*-H···O based on the available structural and spectroscopic data because a large number of oxygen sites (16) defines the inner surface of the structural cage and may act as acceptors of hydrogen bonds. Possibly, the geometry of the H-O-H molecule could be maintained by development of hydrogen bonds between O*1*···*W*···O*2* with distances $d_{O1\text{-}W} \approx 3.21$ Å, $d_{O2\text{-}W} \approx 3.26$ Å and an angle O*1*-*W*-O*2* ≈ 103.93°, which is close to the H-O-H angle in $H_2O$. There are four symmetry equivalent variants for such a $H_2O$ – hydrogen bonded framework interaction.

We assume that water-free fluormayenite was a primary phase in the pyrometamorphic rocks, where a small part of fluorine was already replaced by OH at high temperatures (>900°C). Appearance of $H_2O$ molecules in those structural cages of fluormayenite, which are not occupied by F and OH (*W* sites), is associated with alteration of pyrometamorphic larnite rocks by water vapour-enriched gases. These transformations are related to the thermal history (including combustion process) of the entire rock complex.

Table 9. Calculated powder diffraction data for fluorkyuygenite (1) and fluormayenite (2) (Cu$K\alpha = 1.540598$ Å, Debye-Scherrer geometry, $I > 2$; data were calculated using PowderCell 2.4, Krause & Noltze, 1996) and the synthetic analogue of fluormayenite (3, Costa & Ballirano, 2000).

| | | | *1* | | *2* | | *3* | |
|---|---|---|---|---|---|---|---|---|
| h | k | l | $d_{hkl}$ | $I_{rel.}$ | $d_{hkl}$ | $I_{rel.}$ | $d_{hkl}$ | $I_{rel}$ |
| **2** | **1** | **1** | **4.8851** | **41** | **4.8947** | **92** | **4.887** | **100** |
| 2 | 2 | 0 | 4.2306 | 3 | 4.2389 | 5 | 4.2307 | 4 |
| 3 | 1 | 0 | 3.784 | 7 | 3.7914 | 12 | 3.7852 | 13 |
| **3** | **2** | **1** | **3.1981** | **46** | **3.2043** | **26** | **3.1981** | **32** |
| **4** | **0** | **0** | **2.9915** | **61** | **2.9974** | **47** | **2.9918** | **46** |
| **4** | **2** | **0** | **2.6757** | **100** | **2.6809** | **100** | **2.6755** | **95** |
| 3 | 3 | 2 | 2.5512 | 24 | 2.5562 | 15 | 2.5512 | 18 |
| **4** | **2** | **2** | **2.4426** | **45** | **2.4473** | **43** | **2.4425** | **46** |
| 5 | 1 | 0 | 2.3467 | 17 | 2.3513 | 8 | 2.3465 | 11 |
| **5** | **2** | **1** | **2.1847** | **32** | **2.189** | **41** | **2.1845** | **37** |
| 5 | 3 | 0 | 2.0522 | 8 | 2.0562 | 4 | 2.0519 | 6 |
| 5 | 3 | 2 | 1.9411 | 14 | 1.9449 | 27 | 1.9409 | 25 |
| 6 | 2 | 0 | 1.8920 | 2 | | | | |
| 5 | 4 | 1 | 1.8464 | 2 | 1.85 | 3 | 1.8461 | 3 |
| 6 | 3 | 1 | 1.7643 | 8 | 1.7677 | 5 | 1.764 | 4 |
| 4 | 4 | 4 | 1.7271 | 6 | 1.7305 | 10 | | |
| 7 | 1 | 0 | 1.6923 | 7 | 1.6956 | 6 | 1.6919 | 7 |
| 5 | 4 | 3 | 1.6923 | 5 | | | | |
| **6** | **4** | **0** | **1.6594** | **27** | **1.6626** | **33** | **1.6591** | **25** |
| 6 | 3 | 3 | 1.6284 | 6 | 1.6316 | 5 | 1.628 | 9 |
| 5 | 5 | 2 | | 8 | | | | |
| **6** | **4** | **2** | **1.599** | **26** | **1.6022** | **37** | **1.5987** | **26** |
| 6 | 5 | 1 | 1.5197 | 8 | | | | |
| 7 | 3 | 2 | | 4 | 1.5227 | 4 | 1.5193 | 7 |
| 8 | 0 | 0 | 1.4958 | 4 | 1.4987 | 6 | 1.4954 | 4 |
| 7 | 4 | 1 | 1.4729 | 10 | 1.4758 | 9 | 1.4726 | 6 |
| 8 | 2 | 0 | 1.4511 | 2 | | | | |
| 6 | 5 | 3 | 1.4302 | 3 | | | | |
| 7 | 4 | 3 | 1.391 | 10 | 1.3937 | 10 | 1.3906 | 14 |
| 7 | 5 | 0 | | 6 | | | | |
| 7 | 5 | 2 | 1.3549 | 5 | 1.3575 | 3 | 1.3545 | 2 |
| 8 | 4 | 0 | 1.3378 | 3 | 1.3405 | 7 | 1.3374 | 4 |
| 8 | 4 | 2 | 1.3056 | 3 | 1.3082 | 10 | 1.3052 | 5 |
| 6 | 5 | 5 | 1.2903 | 3 | | | | |
| 6 | 6 | 4 | 1.2756 | 3 | 1.2781 | 5 | 1.2752 | 3 |
| 7 | 5 | 4 | 1.2613 | 2 | 1.2638 | 3 | 1.2610 | 3 |
| 9 | 4 | 1 | 1.2088 | 2 | 1.2111 | 3 | 1.2083 | 3 |
| 8 | 5 | 3 | | | | | | |

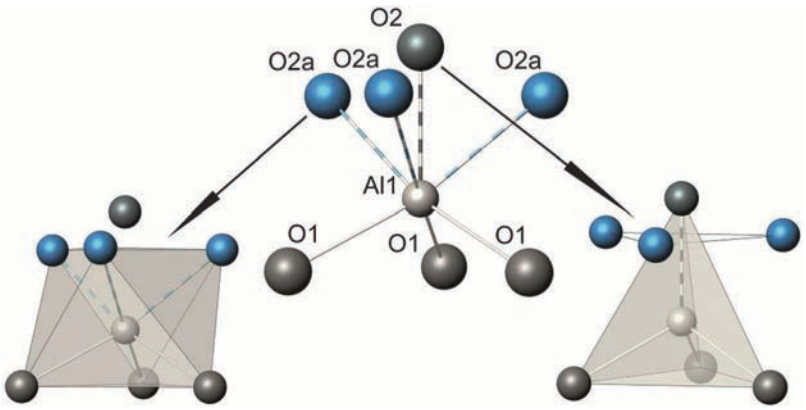


Fig. 6. Al*1* coordination in fluormayenite: 89 % of Al*1* is tetrahedrally coordinated by 3 × O*1* and 1 × O*2* (right side), the remaining 11 % is octahedrally coordinated (left) by 3 × O*1* and 3 × O2*a* where O2*a* is occupied by OH.

Interestingly, this ''kyuygenitization'' process, *i.e*. subsequent incorporation of neutral $H_2O$ molecules into structural cages in minerals of the mayenite group as a result of gaseous metasomatism, protects these minerals from later low-temperature hydration. Appearance of OH groups at the framework oxygen site O2*a* is mainly characteristic of fluormayenite and chlormayenite. Hydroxylation of this type is a consequence of low-temperature hydrothermal alterations widely occurring in pyrometamorphic rocks of the Hatrurim Complex.

**Acknowledgements:** The authors thank Edward Grew for the comments on the first draft version of the manuscript, and two anonymous reviewers for their careful review that improved the early version of the manuscript. The work was partly supported by the National Science Centre (NCN) of Poland, grant no. N N307 100238 and DEC-2012/05/B/ST10/00514 (E.G. & I.G.) and by the Russian Foundation for Basic Researchs, grant no. 12-05-00057 (V.Sh.).

## References

Bentor, Y. (1960): Israel. *in* ''Lexique Stratigraphique International'', vol. III, part 10.2, Asie, 80 p. Centre National de la Recherche Scientifique, Paris.

Britvin, S.N., Murashko, M., Vapnik, Y., Polekhovsky, Y.S., Krivovichev, S.V. (2013a): Halamishite, IMA 2013–105: Negevite, IMA 2013–104; Transjordanite, IMA2013–106; Zuktamrurite, IMA2013–107. CNMNC Newsletter No. 19, February 2014, pages 166–167; *Mineral. Mag.*, **78**, 165–170.

Britvin, S.N., Vapnik, Y., Polekhovsky, Y.S., Krivovichev, S.V. (2013b): Murashkoite, IMA 2012–071. CNMNC Newsletter No. 15, February 2013, page 8. *Mineral. Mag.*, **77**, 1–12.

Costa, U. & Ballirano, P. (2000): Improved powder X-ray data for the cement phase $Ca_{12}Al_{14}O_{32}F_2$ ($C_{11}A_7F$). *Powder Diffr.*, **15**, 56–61.

Dulski, M., Gfeller, F., Marzec, K.M., Kusz, J., Armbruster, T., Galuskina, I.O., Bailau, R., Galuskin, E.V. (2014): A new type of water in natural mayenites – a spectroscopy research. Abstracts of 21st General Meeting of IMA, South Africa, 2014.

Galuskin, E.V., Kusz, J., Armbruster, T., Bailau, R., Galuskina, I.O., Ternes, B., Murashko, M. (2012): Re-investigation of mayenite from the type locality, Ettringer Bellerberg volcano near Mayen (Eifel district, Germany). *Mineral. Mag.*, **76**, 707–716.

Galuskin, E.V., Gfeller, F., Armbruster, T., Galuskina, I.O., Vapnik, Y., Murashko, M., Dzierżanowski, P. (2013a): Fluormayenite, IMA 2013–019. CNMNC Newsletter No. 16, August 2013, page 2705. *Mineral. Mag.*, **77**, 2695–2709.

Galuskin, E.V., Gfeller, F., Armbruster, T., Sharygin, V.V., Galuskina, I.O., Krivovichev, S.V., Vapnik, Y., Murashko, M., Dzierżanowski, P., Wirth, R. (2013b): Fluorkyuygenite, IMA 2013–043. CNMNC Newsletter No. 17, October 2013, page 3000. *Mineral. Mag.*, **77**, 2997–3005.

Galuskin, E.V., Gfeller, F., Armbruster, T., Galuskina, I.O., Vapnik, Ye., Murashko, M., Włodyka, R., Dzierżanowski, P. (2013c): Nabimusaite, IMA 2012–057. CNMNC Newsletter No. 15, February 2013, page 5. *Mineral. Mag.*, **77**, 1–12.

Galuskin, E.V., Gfeller, F., Galuskina, I.O., Armbruster, T., Vapnik, Ye., Włodyka, R., Dzierżanowski, P., Murashko, M. (2013d): Zadovite, IMA 2013–031. CNMNC Newsletter No. 16, August 2013, page 2708; *Mineral. Mag.*, **77**, 2695–2709.

Galuskin, E.V., Galuskina, I.O., Pakhomova, A., Armbruster, T., Vapnik, Y., Dzierżanowski, P., Murashko, M. (2013e): Aradite, IMA 2013–047. CNMNC Newsletter No. 17, October 2013, page 3001. *Mineral. Mag.*, **77**, 2997–3005.

Galuskin, E.V., Galuskina, I.O., Kusz, J., Armbruster, T., Marzec, K.M., Dzierżanowski, P., Murashko, M. (2014): Vapnikite $Ca_3UO_6$ - a new double-perovskite mineral from pyrometamorphic larnite rocks of the Jabel Harmun, Palestinian Autonomy, Israel. *Mineral. Mag.*, **78**, 571–581.

Galuskin, E.V., Gfeller, F., Galuskina, I.O., Armbruster, T., Bailau, R., Sharygin, V.V. (2015a): Mayenite supergroup, part I: Recommended nomenclature. *Eur. J. Mineral.*, **27**, DOI: 10.1127/ejm/2015/0027-2418

Galuskin, E.V., Galuskina, I.O., Kusz, J., Gfeller, F., Armbruster, T., Bailau, R., Dulski, M., Gazeev, V.M., Pertsev, N.N., Zadov, A.E., Dzierżanowski, P. (2015b): Mayenite supergroup, part II: Chlorkyuygenite from northern Caucasus Kabardino-Balkaria, Russia, a new microporous mayenite supergroup mineral with ''zeolitic'' $H_2O$. *Eur. J. Mineral.*, **27**, DOI: 10.1127/ejm/2015/0027-2419

Galuskina, I.O., Vapnik, Y., Prusik, K., Dzierżanowski, P., Murashko, M., Galuskin, E.V. (2013): Gurimite, IMA 2013–032. CNMNC Newsletter No. 16, August 2013, page 2708. *Mineral. Mag.*, **77**, 2695–2709.

Galuskina, I.O., Vapnik, Ye., Lazic, B., Armbruster, T., Murashko, M., Galuskin, E.V. (2014): Harmunite $CaFe_2O_4$: a new mineral from the Jabel Harmun, West Bank, Palestinian Autonomy, Israel. *Am. Mineral.*, **99**, 965–975.

Garcia, C.S., Abedinb, M.N., Sharmac, S.K., Misrac, A.K., Ismailb, S., Singhb, U., Refaata, T.F., Elsayed-Alia, H., Sandfordb, S. (2006): Remote pulsed laser Raman spectroscopy system for detecting water, ice, and hydrous minerals. Proc. SPIE 6302, *Imaging Spectrometry* XI, 630215 (1 September 2006), doi: 10.1117/12.680879.

Geller, Y.I., Burg, A., Halicz, L., Kolodny, Y. (2012): System closure during the combustion metamorphic ''Mottled Zone'' event, Israel. *Chem. Geol.*, **334**, 25–36.

Gfeller, F., Środek, D., Kusz, J., Dulski, M., Gazeev, V., Galuskina, I., Galuskin, E., Armbruster, T. (2015): Mayenite supergroup, part IV: Crystal structure and Raman investigation of Al-free eltyubyuite from the Shadil-Khokh volcano, Kel' Plateau, Southern Ossetia, Russia. *Eur. J. Mineral.*, **27**, DOI: 10.1127/ejm/2015/0027-2421

Gross, S. (1977): The mineralogy of the Hatrurim formation, Israel. *Geol. Surv. Isr. Bull.*, **70**, 80 p.

Hayashi, K., Hirano, M., Hosono, H. (2005): Thermodynamics and kinetics of hydroxide ion formation in $12CaO \cdot 7Al_2O_3$. *J. Phys. Chem.*, **109**, 11900–11906.

Hentschel, G. (1964): Mayenit, $12CaO{\cdot}7Al_2O_3$, und Brownmillerit, $2CaO{\cdot}(Al,Fe)_2O_3$, zwei neue Minerale in den Kalksteineinschlüssen der Lava des Ettringer Bellerberges. *N. Jb. Mineral. Mh.*, **1964**, 22–29.

Huang, K.-W., Chen, W.-T., Chu, C.-I., Hu, S.-F., Sheu, H.-S., Cheng, B.-M., Chen, J.-M., Liu, R.-S. (2012): Controlling the

activator site to tune europium valence in oxyfluoride phosphors. *Chem. Mater.*, **24**, 2220–2227.

Kolesov, B. (2006): Raman investigation of $H_2O$ molecule and hydroxyl groups in the channels of hemimorphite. *Am. Mineral.*, **91**, 1355–1362.

Krause, W. & Nolze, G. (1996): Powder Cell - a program for the representation and manipulation of crystal structures and calculation of the resulting X-ray powder patterns. *J. Appl. Crystallogr.*, **29**, 301–303.

Mandarino, J.A. (1979): The Gladstone-Dale relationship. Part III: 28 some general applications. *Can. Mineral.*, **17**, 71–76.

Murashko, M.N., Chukanov, N.V., Mukhanova, A.A., Vapnik, E., Britvin, S.N., Polekhovsky, Yu.S., Ivakin, Yu.D. (2011): Barioferrite $BaFe_{12}O_{19}$: A new mineral species of the magnetoplumbite group from the Hatrurim formation in Israel. *Geol. Ore Dep.*, **57**, 558–563.

Novikov, I., Vapnik, Y., Safonova, I. (2013): Mud volcano origin of the Mottled Zone, South Levant. *Geosci. Front.*, **4**, 597–619.

Qujiun, Y., Sugita, S., Xiuji, F., Mi, J. (1997): On the preparation of single crystal of $11CaO \cdot 7Al_2O_3 \cdot CaF_2$ and the confirmation of its structure. *Cem. Concr. Res.*, **27**, 1439–1449.

Sango, H. (2006): Ion-exchange characteristics of $12CaO \cdot 7Al_2O_3$ for halide and hydroxyl ions. *J. Eur. Ceram. Soc.*, **26**, 803–807.

Sharygin, V.V., Lazic, B., Armbruster, T.M., Murashko, M.N., Wirth, R., Galuskina, I.O., Galuskin, E.V., Vapnik, Ye., Britvin, S.N., Logvinova, A.M. (2013): Shulamitite $Ca_3TiFe^{3+}AlO_8$ – a new perovskite-related mineral from Hatrurim Basin, Israel. *Eur. J. Mineral.*, **25**, 97–111.

Sheldrick, G.M. (2008): A short history of SHELX. *Acta Crystallogr.*, **A64**, 112–122.

Sokol, E.V., Novikov, I.S., Vapnik, Ye., Sharygin, V.V. (2007): Gas fire from mud volcanoes as a trigger for the appearance of high temperature pyrometamorphic rocks of the Hatrurim Formation (Dead Sea area). *Dokl. Earth Sci.*, **413A**(3), 474–480.

Sokol, E.V., Novikov, I.S., Zateeva, S.N., Sharygin, V.V., Vapnik, Ye. (2008): Pyrometamorphic rocks of the spurrite-merwinite facies as indicators of hydrocarbon discharge zones (the Hatrurim Formation, Israel). *Dokl. Earth Sci.*, **420**(4), 608–614.

Vapnik, Ye., Sharygin, V.V., Sokol, E.V., Shagam, R. (2007): Paralavas in a combustion metamorphic complex: Hatrurim Basin, Israel. *Rev. Eng. Geol.*, **18**, 1–21.

Williams, P.P. (1973): Refinement of structure of $11CaO \cdot 7Al_2O_3$?$CaF_2$. *Acta Crystallogr.*, **B29**, 1550–1551.

*Received 7 July 2014*
*Modified version received 11 October 2014*
*Accepted 21 October 2014*